ACS Macro Letters

pubs.acs.org/macroletters Letter

Combining Metal-Free and Metal-Mediated Ring-Opening Metathesis Polymerization for Efficient Synthesis of Bottlebrush Polymers

Margaret E. Tetzloff and Andrew J. Boydston*

Cite This: ACS Macro Lett. 2025, 14, 983−988 Read Online

ACCESS | Metrics & More | Article Recommendations | Supporting Information

ABSTRACT: Metal-mediated ring-opening metathesis polymerization (ROMP) is a common tool used to synthesize the backbone of bottlebrush polymers by a graft-through approach. However, examples of ROMP oligomers or polymers as macromolecular side chains are limited due in part to the challenges associated with preparing a macromonomer via the same polymerization mechanism as the one used to create the main chain. Accordingly, installation of polymerizable units onto macromonomers produced via ROMP has been achieved in a multistep fashion. In such cases, one metal initiator is used in the preparation of each macromonomer, thus constituting an overall usage of the metal complex that is 1:1 with repeat units in the final bottlebrush polymer product. By leveraging the modularity of organic initiators in metal-free ROMP (MF-ROMP), as well as the differences in monomer selectivities between metal-mediated ROMP and MF-ROMP, we demonstrate a uniquely efficient and low-metal-use route to bottlebrush polymers. Specifically, we found that norbornene imide-functionalized vinyl ether initiators were successful in MF-ROMP to produce macromonomers from tetracyclododecene without compromising the norbornene imide unit. Subsequent metal-mediated graft-through ROMP of the norbornene imide chain end using Grubbs' third-generation catalyst then produced high-molecular-weight bottlebrush copolymers. We report the synthetic methods for this sequential ROMP−ROMP approach, comparative analyses for *endo*- and *exo*-isomers of the macromonomers, and thermal characterization of the bottlebrush polymers.

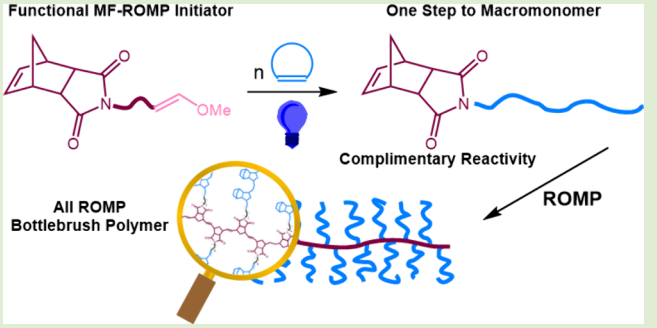

Bottlebrush polymers (BBPs) make up a structurally interesting class of copolymers defined by their series of macromolecular side chains connected by a polymeric backbone. Beyond the specific side chain and backbone compositions, additional degrees of freedom in terms of bottlebrush structure include the molecular weight of the side chains (M_{SC}) and backbone (M_{BB}), as well as the grafting density. These features can be tuned using a variety of well-controlled polymerization strategies to produce highly tailorable macromolecules and functional materials.[1] In particular, BBPs with a high grafting density of side chains can display unique properties as a result of their highly strained geometries.[2] The rigidity and steric repulsion of these BBPs result in a macromolecule with few entanglements, which have found use in applications from viscosity modification[3] to drug delivery.[4,5]

Advancements in methods for polymerization of macromonomers (MMs) in a graft-through fashion are of particular interest because they achieve 100% grafting density and can do so from well-defined MM structures.[6] ROMP of MMs using the Grubbs third-generation initiator (G3) has been widely useful for polymerization of norbornene-functionalized MMs, in large part because G3 displays high rates of polymerization, broad functional group tolerance, and nearly quantitative conversion of monomer.[7] The norbornenyl end group can either be installed on a macromonomer as a postpolymerization modification reaction, or by being present during the polymerization process as a part of the initiator[8] or a chain-transfer agent,[9] as long as the strained cyclic olefin is unreactive toward the first polymerization mechanism. Making densely grafted BBPs utilizing ROMP has resulted in a wide variety of macromolecules with diversity across their side-chain identity,[7] anchor group,[10,11] size,[12,13] and side-chain functionality.[14] Typically, polymerizations that display living characteristics and good chain-end fidelity are used to produce the macromonomers. Examples include atom-transfer radical

Received: May 6, 2025
Revised: June 5, 2025
Accepted: June 16, 2025
Published: June 30, 2025

https://doi.org/10.1021/acsmacrolett.5c00300
ACS Macro Lett. 2025, 14, 983−988

polymerization,[15] reversible addition−fragmentation chain transfer polymerization,[16] and ring-opening polymerization.[17]

Although ROMP is also a well-controlled polymerization, it is usually confined to its use in bottlebrush polymer backbone synthesis and is rarely used to make side chains due to synthetic challenges. Kiessling and co-workers nicely addressed synthetic challenges of using metal-mediated ROMP at two distinct stages of the bottlebrush polymer synthesis by using a grafting-from approach to all-ROMP polymers.[18] Alternatively, graft-through approaches are attractive, because they ensure 100% grafting density. This approach is also rare for sequential ROMP−ROMP methods. Inherent in the use of a metal−alkylidene initiator to make an MM is the fact that it has to be removed and exchanged for a norbornene chain end (or similarly ROMP-compatible moiety). For example, MM synthesis using ROMP has been achieved by Kilbinger and co-workers[19] and more recently by Johnson and co-workers[20] using Grubbs-type metathesis catalysts (Figure 1). In each scenario, macromonomers were synthesized and then a series of postpolymerization chain-end modification steps were used to access the desired macromonomer. Although these two examples clearly displayed successful access to ROMP−ROMP BBPs, two important considerations are noted. First, sequences of chain-end modifications can result in less than 100% chain-end functionalization. Second, each macromonomer uses a stoichiometric amount of metal−alkylidene (one per macromonomer), resulting in a final BBP that necessitates one metal complex per repeat unit in the backbone. Efficient access to ROMP−ROMP BBPs is desirable because the rigidity of having a norbornene-based ROMP polymer as a side chain has shown promise for making interesting materials. For example, Johnson and co-workers noted that self-assembly of Janus diblock BBPs with ROMP side chains resulted in larger domain spacings as compared to commonly employed polystyrene side chains of similar molecular weight. A more streamlined approach to ROMP−ROMP BBP synthesis could allow for broader applications of these materials, especially in fields of use where metal-based reagents are limited from either cost or contamination viewpoints.

Instead of a transition-metal-based initiator, one variant of metal-free ROMP (MF-ROMP, Scheme 1) can employ an organic initiator such as **1**, but with modularity of the R and R' groups (Scheme 1).[21−24] We envisioned the use of tailored enol ether initiators (e.g., **2a**/**2b**) to enable the strategic installation of functional groups at the chain end, thereby producing hemitelechelic ROMP polymers in a single step and ensuring 100% chain-end functionalization with the norbornene imide (NBI). Of course, this requires that the chain-end functional group does not display deleterious reactivity under the conditions of MF-ROMP. Here, we found opportunity in "failure." Specifically, MF-ROMP is thus far incapable of polymerizing NBI monomers for reasons that are not yet understood. On the one hand, the inability to use NBIs in MF-ROMP is unfortunate considering their great utility across multiple ROMP studies and applications. On the other hand,

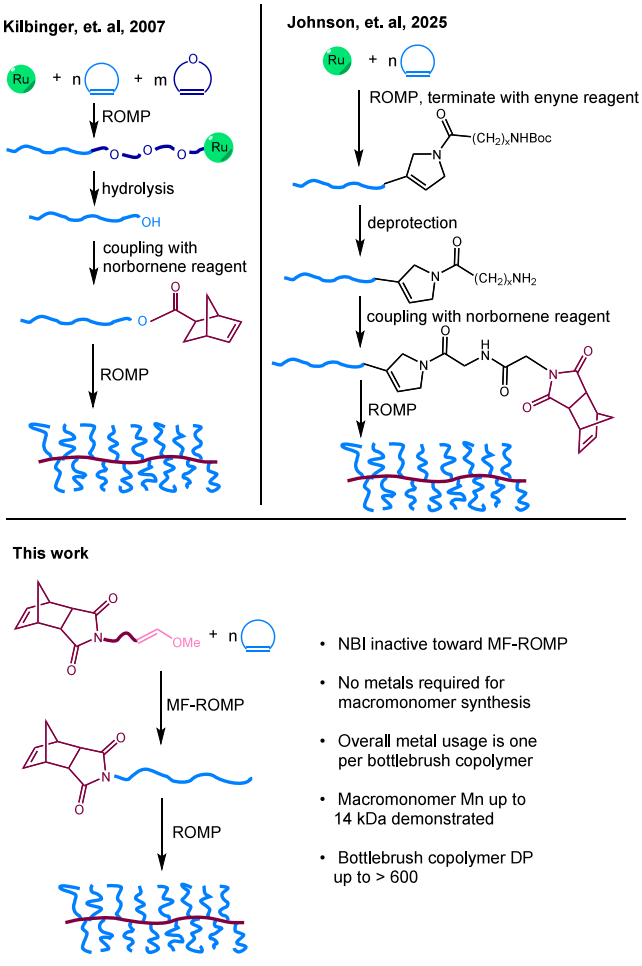

Figure 1. Approaches to graft-through all-ROMP bottlebrush polymers. (Top) Previous metal-mediated strategies for ROMP-derived macromonomer synthesis involving removal of metal alkylidene and subsequent installation of a norbornenyl chain end. (Bottom) Macromonomer synthesis by functional MF-ROMP initiators presented in this work.

Scheme 1. (Top) Simplified Mechanism for MF-ROMP; (Bottom) Initiators, Monomer, and Photocatalyst Used in MF-ROMP

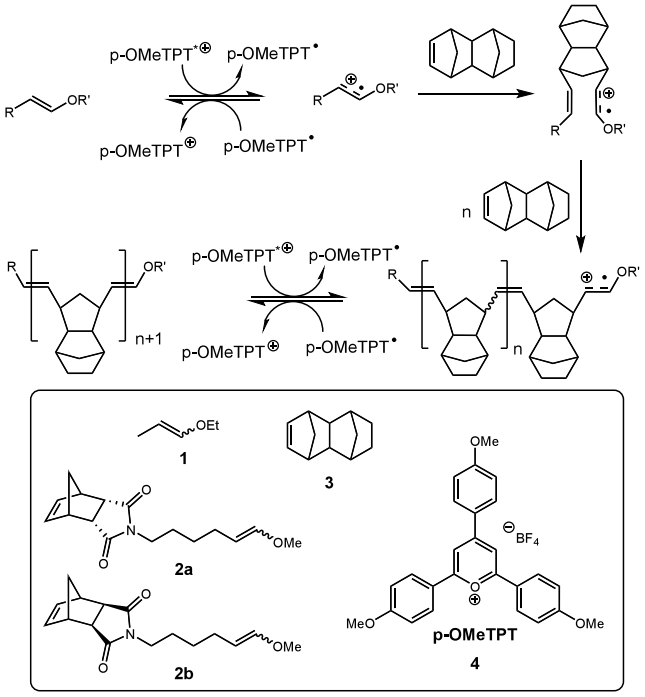

https://doi.org/10.1021/acsmacrolett.5c00300
ACS Macro Lett. 2025, 14, 983−988

Table 1. Summary of MMs Synthesized by MF-ROMP

entry	polymer	initiator	[M]:[I]	conv.[a] (%)	M_n[b] (kDa)	$Đ$[c]	initiator efficiency[d] (%)
1	*endo*-$MM_{2.5}$	**2a**	8:1	64	2.52	1.27	32
2	*endo*-$MM_{3.5}$	**2a**	9:1	84	3.53	1.45	34
3	*endo*-$MM_{3.8}$	**2a**	10:1	92	3.82	1.41	39
4	*endo*-$MM_{5.3}$	**2a**	11:1	97	5.29	1.63	32
5	*endo*-MM_{6}	**2a**	12:1	96	6.04	1.67	30
6	*endo*-$MM_{9.6}$	**2a**	30:1	91	9.57	1.49	46
7	*exo*-$MM_{5.6}$	**2b**	12:1	83	5.60	1.42	30
8	*exo*-MM_{6}	**2b**	13:1	88	5.95	1.35	31
9	*exo*-MM_{10}	**2b**	30:1	84	9.92	1.24	41
10	*exo*-MM_{14}	**2b**	70:1	70	13.95	1.48	56
11	*exo*-MM_{20}	**2b**	80:1	72	20.43	1.49	45

[a]Conversion of **3**, as determined by ^{1}H NMR analysis. [b]Experimental number-average molecular weight calculated from the experimental weight-average molecular weight determined by GPC using MALS. [c]Dispersities determined by GPC analysis. [d]Initiator efficiency calculated using theoretical M_n based on NMR conversion and M_n determined by GPC.

Table 2. Summary of Results from Graft-through ROMP to Form Bottlebrush Polymers

entry	MM	[MM]:[G3]	conv[a] (%)	M_n of BBP[b] (kDa)	DP of BBP[c]	$Đ$ of BBP[b,d]	IE[e] (%)
1	*endo*-$MM_{2.5}$	10:1	≥95	478	190	1.71	5
2	*endo*-$MM_{3.5}$	25:1	66	2290	649	1.27	3
3	*endo*-$MM_{3.8}$	10:1	≥95	251	65.7	2.36	14
4	*endo*-$MM_{5.3}$	10:1	79	240	45.4	1.54	17
5	*endo*-MM_{6}	10:1	≥95	42.9	7.10	1.59	133
6	*endo*-MM_{6}	25:1	47	132	21.9	1.34	53
7	*endo*-MM_{6}	50:1	10	161	26.7	1.44	19
8	*endo*-$MM_{9.6}$	25:1	0				
9	*exo*-$MM_{5.6}$	25:1	≥95	563	101	1.68	24
10	*exo*-$MM_{5.6}$	50:1	≥95	2550	455	1.35	10
11	*exo*-MM_{6}	10:1	≥95	168	30	2.63	34
12	*exo*-MM_{6}	25:1	≥95	691	123	2.09	21
13	*exo*-MM_{6}	50:1	≥95	2280	407	1.27	12
14	*exo*-MM_{6}	75:1	≥95	3350	598	1.13	13
15	*exo*-MM_{6}	100:1	≥95	3980	710	1.11	14
16	*exo*-MM_{10}	50:1	93	1040	105	1.68	45
17	*exo*-MM_{14}	50:1	92	688	49.3	1.89	94
18	*exo*-MM_{20}	50:1	0				

[a]Conversion was calculated by integrating the GPC peak areas from the RI detector. [b]Experimental number-average molecular weight calculated from the experimental weight-average molecular weight determined by GPC using MALS. [c]Degree of polymerization was calculated by dividing M_n of BBP by M_n of MM. [d]Dispersities determined by GPC analysis. [e]Initiator efficiency (IE) was calculated using theoretical M_n based on GPC conversion and M_n determined by GPC.

this presented an opportunity to leverage the complementarity of MF-ROMP and metal-mediated ROMP. With these goals in mind, we envisioned a method of ROMP−ROMP BBP synthesis that exchanged the need for transition-metal catalysts in MM production for organic initiators that contain a ROMP-able NBI functionality that is unreactive during MF-ROMP. This approach would eliminate the need for the postpolymerization installation of a norbornene chain end prior to BBP synthesis. Using MF-ROMP, MM synthesis can be streamlined, and the number of transition metal complexes needed per BBP chain can be reduced from one per MM (plus one for the BBP main chain) down to one overall.

RESULTS AND DISCUSSION

Building from empirical observations that NBI monomers were not incorporated into polymer chains during MF-ROMP, even as a comonomer with norbornene, we wanted to investigate the use of NBIs in custom initiators for MF-ROMP. Toward this end, we synthesized *endo*- and *exo*-isomers of NBI initiators (**2a** and **2b**, respectively) starting from the corresponding carbic anhydride isomers. Initiators **2a** and **2b** were each produced in a 23% overall yield, assuming the highest isolated yield for each step. Briefly, the reaction sequence involved imide formation, alcohol oxidation using Dess-Martin periodinane, and the Wittig reaction to install the vinyl ether functionality.

With initiators **2a** and **2b** at hand, we next investigated their performance in MF-ROMP of tetracyclododecene (TD) **3** (Table 1). We chose TD based on its demonstrated compatibility with MF-ROMP, resistance to chain transfer during metal-mediated ROMP, ability to provide valuable materials with high glass transition temperatures (T_g),[25] and industrial relevance. MF-ROMP of TD was performed under an ambient atmosphere using pyrylium photocatalyst **4** in a 1:1 v/v mixture of CH_2Cl_2 and 1,2-dichlorobenzene with blue light irradiation for 1 h. We found that each functional initiator (**2a** and **2b**) formed oligo- and polyTD MMs with comparable conversions, initiator efficiencies, and molecular weight dispersities ($Đ$) as those observed in previous reports that

https://doi.org/10.1021/acsmacrolett.5c00300
ACS Macro Lett. 2025, 14, 983−988

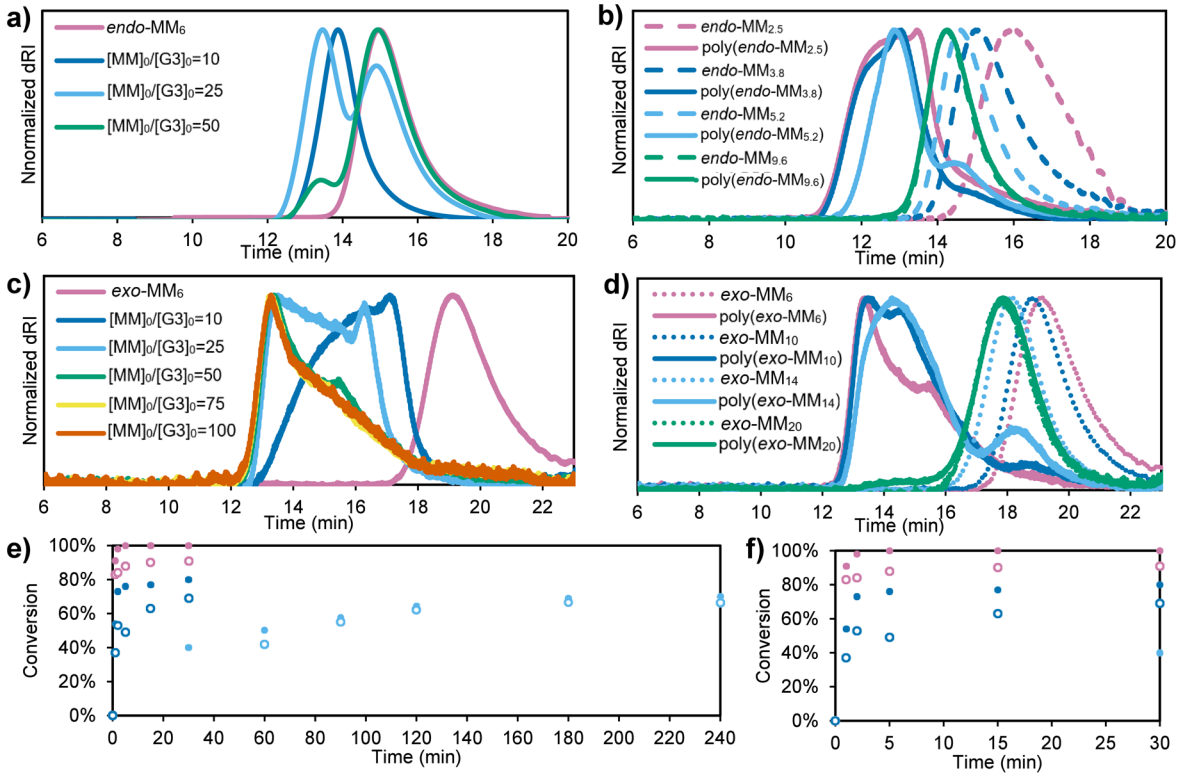

Figure 2. (a) GPC (THF) traces of *endo*-MM_6 and crude polymerization products at varying $[MM]_0/[G3]_0$. (b) GPC (toluene) traces of *endo*-MMs of varying sizes and the corresponding crude polymerization products at $[MM]_0/[G3]_0$ = 10. (c) GPC (toluene) traces of *exo*-MM_6 and crude polymerization products at varying $[MM]_0/[G3]_0$. (d) GPC (toluene) traces of *exo*-MMs of varying sizes and corresponding crude polymerization products at $[MM]_0/[G3]_0$ = 50. (e, f) ROMP conversion of *endo*-$MM_{3.5}$ ($[MM]_0/[G3]_0$ = 25, light blue) and *exo*-$MM_{5.6}$ ($[MM]_0/[G3]_0$ = 25, pink; $[MM]_0/[G3]_0$ = 50, dark blue) by GPC (filled circles) and NMR (empty circles) analysis over time.

used ethyl propenyl ether (**1**) as the initiator.[21,26] It was confirmed by ^{1}H NMR spectroscopy using 1,2 dichloroethane as an internal standard that the alkene signals in the NBI at δ = 6.08 and 6.28 ppm for **2a** and **2b**, respectively, did not change over the course of the MF-ROMP and remained intact after purification by precipitation into cold methanol (Figures S1–S4). The integration of the NBI alkene relative to polymer backbone alkenes also agreed well with the number-average degree of polymerization (DP) determined by gel permeation chromatography (GPC) with toluene as a mobile phase. MMs of different molecular weights were prepared by manipulating the feed ratio of monomer and initiator to yield the target MM, denoted as *endo*-MM_n and *exo*-MM_n, with the subscript indicating the number-average molecular weight (M_n) in kDa (Table 1).

We next carried the series of MMs into graft-through polymerization experiments using G3 (Table 2). We first wanted to understand the extent of backbone polymerization that could be achieved with this method. For direct comparisons, ROMP of *endo*-MM_6 (Table 2, entries 5–7) and *exo*-MM_6 (Table 2, entries 11–13) were carried out in a nitrogen-filled glovebox using initial $[MM]_0$:$[G3]_0$ ratios of 10, 25, and 50 to 1 (Figure 2a,c). We found that the *endo*-isomer was challenged to achieve BBPs with high DP, as has generally been observed for *endo*-isomers in ROMP and especially in the case of graft-through BBP syntheses.[27,28] Only the polymerization that used a 10:1 $[MM]_0$:$[G3]_0$ (Table 2, entry 5) reached full conversion of the MM, as assessed by GPC analysis. Attempts at using higher $[MM]_0$:$[G3]_0$ (>50:1) with the *endo*-MM resulted in bimodal GPC traces, with the longer retention time peak corresponding to unreacted MM. To the contrary, ROMP of *exo*-MM_6 achieved conversions of >90% even at $[MM]_0$:$[G3]_0$ of 100 to 1 (Table 2, entries 14 and 15). Dispersities for the bottlebrush polymers were high compared to other ROMP of small molecules and MMs synthesized by living polymerizations. However, this is somewhat unsurprising considering BBPs reflect the propagation of dispersity through each step of their synthesis.[29] While we can expect a relatively low dispersity in M_{BB}, the side chains reflect the moderate dispersities common in MF-ROMP (1.30–1.60). The M_n of the resultant BBPs was consistently found to be greater than the theoretical M_n, giving a calculated initiator efficiency of <1. We also note that in general the GPC traces of the BBPs show signs of aggregation. We speculate that some deactivation of the G3 initiator may occur from reaction with residual enol ether. That said, we also note that the initiator efficiency of G3 does not trend consistently with changes in $[MM]_0$:$[G3]_0$, and it is therefore difficult to deconvolute the chemical reactivity origins of low initiator efficiency from mass transport phenomena.

Experiments comparing the time to reach high conversion were carried out for both *endo*- and *exo*-MMs at a $[MM]_0$:$[G3]_0$ ratio of 25 to 1, as well as 50:1 for *exo*-MMs (Figure 2e,f). Conversion was measured by both ^{1}H NMR spectroscopy and GPC. The signal-to-noise ratio for GPC analysis was higher than that of ^{1}H NMR analysis of the MM chain end and is likely a more accurate assessment of conversion. GPC results also likely underestimate conversion, as there is a slight overlap in MM and BBP peaks. Although the polymerization did not display living characteristics and deviated from linear pseudo-

https://doi.org/10.1021/acsmacrolett.5c00300
ACS Macro Lett. 2025, 14, 983–988

first order kinetics (Figures S7−S9), we were interested in the rate of reaction since slower propagation in ROMP of MMs has commonly resulted in reduced conversion.[11] The same trend was observed here, with *endo*-$MM_{3.5}$ reaching a final conversion of 66% by GPC after 4 h, whereas *exo*-$MM_{5.6}$ was able to achieve nearly quantitative conversion within 30 min. Next, we explored the effect of M_{SC} on conversion in graft-through ROMP. Each isomeric variant displayed a strong dependence on the M_{SC}, with the *endo*-MMs reaching high conversions only when the M_{SC} was less than 6 kDa and low $[MM]_0$:$[G3]_0$ was employed (Figure 2b,d). When *endo*-$MM_{9.6}$ was used with a $[MM]_0$:$[G3]_0$ of 10:1, no BBP was detected by GPC analysis. Interestingly, the ROMP of *exo*-MM_ns proceeded smoothly, even with a M_{sc} = 14 kDa and $[MM]_0$:$[G3]_0$ = 50:1. Increasing the M_{sc} to *exo*-MM_{20}, however, resulted in no BBP polymer according to GPC analysis.

We also wanted to explore the effect of ROMP−ROMP on the thermal properties of the polymers. Though the MMs were soluble in THF, high molecular weight BBPs were discovered to be insoluble in THF, and could be purified by precipitating into cold THF to yield the high molecular weight BBP with high purity, as determined by ^{1}H NMR and GPC analysis (Figures S26 and S27). We also synthesized analogous linear polymers of TD by polymerization with the Grubbs first-generation initiator with molecular weights comparable to the bottlebrush polymers. We compared *exo*-MM_6, two sizes of BBPs, and linear polyTD analogues via differential scanning calorimetry (DSC) (Figure 3).

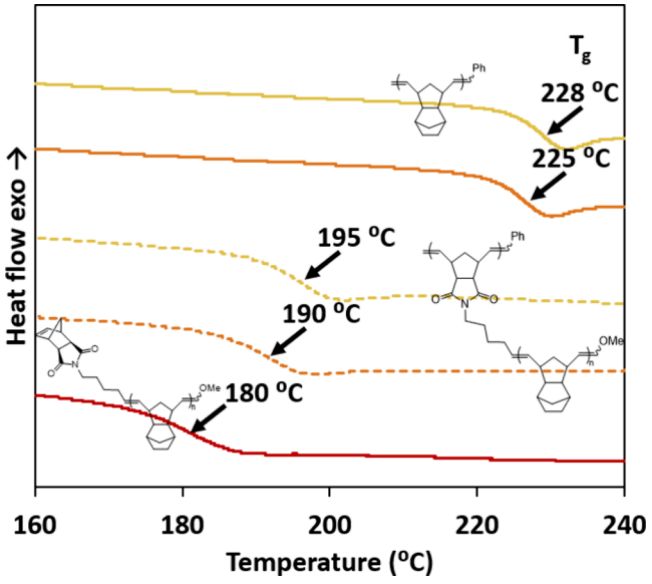

Figure 3. Experimental T_g data of *exo*-MM_6 (red), BBP (dotted traces) at M_ns 212 (orange) and 916 kDa (yellow), and analogous linear pTD (solid traces) at 289 (orange) and 729 kDa (yellow).

Although both BBPs and linear analogues had T_g values higher than *exo*-MM_6 due to being significantly higher in molecular weight, the T_g values of BBPs were lower than their linear analogues by 30 to 35 °C. This is consistent with other such comparisons and is ascribed to an increase in the available free volume and, consequently, increased segmental motion as a result of the increase in the number of chain ends.[3,30−32]

CONCLUSIONS

We have demonstrated the application of functional initiators in MF-ROMP and leveraged the complementarity of metal-free versus metal-mediated ROMP to produce ROMP−ROMP BBPs. NBI-functionalized enol ethers of *endo*- and *exo*-variants were used successfully as initiators in MF-ROMP without any measurable ring-opening of the NBI moiety. After purification, these MMs could be directly polymerized with G3 to form BBPs. We identified a strong dependence of conversion on M_{SC} for both *endo*- and *exo*-MMs, as well as an upper limit to the achievable graft-through DP for *endo*-MMs, whereas graft-through polymerization of *exo*-MMs was able to achieve high conversion even at a $[MM]_0$:$[G3]_0$ of 100:1. We found that the T_g values of BBPs increased with increasing M_n, though they are 30 to 35 °C lower than linear polyTD analogs of a similar molecular weight. The ease of MM synthesis and reduction of G3 catalyst required for BBP formation makes this a potentially useful approach for the synthesis of ROMP−ROMP polymers. Additionally, functional initiators in MF-ROMP present an efficient new approach to the chain-end functionalization of ROMP products.

ASSOCIATED CONTENT

Supporting Information

The Supporting Information is available free of charge at https://pubs.acs.org/doi/10.1021/acsmacrolett.5c00300.

Experimental procedures, conversion calculations, detailed polymerization results, and GPC and NMR data (PDF)

AUTHOR INFORMATION

Corresponding Author

Andrew J. Boydston − *Department of Chemistry, University of Wisconsin−Madison, Madison, Wisconsin 53706, United States; Department of Chemical and Biological Engineering and Department of Materials Science and Engineering, University of Wisconsin-Madison, Madison, Wisconsin 53706, United States;* orcid.org/0000-0001-7192-4903; Email: aboydston@wisc.edu

Author

Margaret E. Tetzloff − *Department of Chemistry, University of Wisconsin−Madison, Madison, Wisconsin 53706, United States*

Complete contact information is available at: https://pubs.acs.org/10.1021/acsmacrolett.5c00300

Notes

The authors declare the following competing financial interest(s): A.J.B. has an ownership interest in BCI, Inc., which has licensed technology related to the work disclosed in the manuscript.

ACKNOWLEDGMENTS

We thank Promerus LLC for their generous gift of tetracyclododecene. We gratefully acknowledge financial support from the National Science Foundation (CHE-2002886) and BCI, Inc. A.J.B. acknowledges partial financial support from the Yamamoto Family, the Office of the Vice Chancellor for Research and Graduate Education at the University of Wisconsin − Madison with funding from the Wisconsin Alumni Research Foundation. The Bruker Avance

III 400 MHz NMR spectrometers were supported by the NSF (CHE-1048642) and UW-Madison Instructional Laboratory Modernization Award and the UW-Madison Department of Chemistry. The Bruker Avance III 500 MHz NMR spectrometer was supported by a generous gift from Paul J. and Margaret M. Bender.

REFERENCES

(1) Sheiko, S. S.; Sumerlin, B. S.; Matyjaszewski, K. Cylindrical Molecular Brushes: Synthesis, Characterization, and Properties. *Prog. Polym. Sci.* **2008**, *33*, 759−785.
(2) Sunday, D. F.; Burns, A. B.; Martin, T. B.; Chang, A. B.; Grubbs, R. H. Relationship between Graft Density and the Dilute Solution Structure of Bottlebrush Polymers: An Inter-chemistry Comparison and Scaling Analysis. *Macromolecules* **2023**, *56*, 7419−7431.
(3) Abbasi, M.; Faust, L.; Wilhelm, M. Comb and Bottlebrush Polymers with Superior Rheological and Mechanical Properties. *Adv. Mater.* **2019**, *31*, No. 1806484.
(4) Johnson, J. A.; Lu, Y. Y.; Burts, A. O.; Lim, Y.; Finn, M. G.; Koberstein, J. T.; Turro, N. J.; Tirrell, D. A.; Grubbs, R. H. Core-Clickable PEG-*Branch*-Azide Bivalent-Bottle-Brush Polymers by ROMP: Grafting-Through and Clicking-To. *J. Am. Chem. Soc.* **2011**, *133*, 559−566.
(5) Ohnsorg, M. L.; Prendergast, P. C.; Robinson, L. L.; Bockman, M. R.; Bates, F. S.; Reineke, T. M. Bottlebrush Polymer Excipients Enhance Drug Solubility: Influence of End-Group Hydrophilicity and Thermoresponsiveness. *ACS Macro Lett.* **2021**, *10*, 375−381.
(6) Choinopoulos, I. Grubbs' and Schrock's Catalysts, Ring Opening Metathesis Polymerization and Molecular Brushes—Synthesis, Characterization, Properties and Applications. *Polymers.* **2019**, *11*, 298.
(7) Xia, Y.; Kornfield, J. A.; Grubbs, R. H. Efficient Synthesis of Narrowly Dispersed Brush Polymers via Living Ring-Opening Metathesis Polymerization of Macromonomers. *Macromolecules* **2009**, *42*, 3761−3766.
(8) Fu, Q.; Ren, J. M.; Qiao, G. G. Synthesis of Novel Cylindrical Bottlebrush Polypseudorotaxane via Inclusion Complexation of High Density Poly(ε-caprolactone) Bottlebrush Polymer and α-Cyclodextrins. *Polym. Chem.* **2012**, *3*, 343−351.
(9) Cheng, C.; Khoshdel, E.; Wooley, K. L. One-Pot Tandem Synthesis of a Core−Shell Brush Copolymer from Small Molecule Reactants by Ring-Opening Metathesis and Reversible Addition−Fragmentation Chain Transfer (Co)polymerizations. *Macromolecules* **2007**, *40*, 2289−2292.
(10) Radzinski, S. C.; Foster, J. C.; Chapleski, R. C.; Troya, D.; Matson, J. B. Bottlebrush Polymer Synthesis by Ring-Opening Metathesis Polymerization: The Significance of the Anchor Group. *J. Am. Chem. Soc.* **2016**, *138*, 6998−7004.
(11) Scannelli, S. J.; Alaboalirat, M.; Troya, D.; Matson, J. B. Influence of the Norbornene Anchor Group in Ru-Mediated Ring-Opening Metathesis Polymerization: Synthesis of Bottlebrush Polymers. *Macromolecules* **2023**, *56*, 3838−3847.
(12) Miyake, G. M.; Piunova, V. A.; Weitekamp, R. A.; Grubbs, R. H. Precisely Tunable Photonic Crystals From Rapidly Self-Assembling Brush Block Copolymer Blends. *Angew. Chem., Int. Ed.* **2012**, *51* (45), 11246−11248.
(13) Seo, H. B.; Yu, Y. G.; Chae, C. G.; Kim, M. J.; Lee, J. S. Synthesis of Ultrahigh Molecular Weight Bottlebrush Block Copolymers of ω-end-norbornyl Polystyrene and Polymethacrylate Macromonomers. *Polymer* **2019**, *177*, 241−249.
(14) Yu, X.; Wang, Y.; Li, M.; Zhang, Y.; Huang, Y.; Qian, Q.; Zheng, Y.; Hou, Q.; Fan, X. Self-Healable, Stretchable, and Super-Soft Bottlebrush Polyester Elastomers for Highly Sensitive Flexible Sensors. *ACS Appl. Polym. Mater.* **2023**, *5*, 2750−2759.
(15) Charvet, R.; Novak, B. M. One-Pot, One-Catalyst Synthesis of Graft Copolymers by Controlled ROMP and ATRP Polymerizations. *Macromolecules* **2004**, *37*, 8808−8811.
(16) Patton, D. L.; Advincula, R. C. A Versatile Synthetic Route to Macromonomers via RAFT Polymerization. *Macromolecules* **2006**, *39*, 8674−8683.
(17) McCleary-Petersen, K. C.; Feng, Y.; Guironnet, D. Effect of Macromonomer Chemical Structure on the Rate of Grafting-Through Ring-Opening Metathesis Polymerization. *Polym. Chem.* **2025**, *16*, 217−222.
(18) Allen, M. J.; Wangkanont, K.; Raines, R. T.; Kiessling, L. L. ROMP from ROMP: A New Approach to Graft Copolymer Synthesis. *Macromolecules* **2009**, *42* (12), 4023−4027.
(19) Hilf, S.; Kilbinger, A. F. M. An All-ROMP Route to Graft Copolymers. *Macromol. Rapid Commun.* **2007**, *28*, 1225−1230.
(20) Sun, Z.; Liu, B.; Ma, M.; Alexander-Katz, A.; Ross, C. A.; Johnson, J. A. ROMP of Macromonomers Prepared by ROMP: Expanding Access to Complex, Functional Bottlebrush Polymers. *J. Am. Chem. Soc.* **2025**, *147*, 3855.
(21) Ogawa, K. A.; Goetz, A. E.; Boydston, A. J. Metal-Free Ring-Opening Metathesis Polymerization. *J. Am. Chem. Soc.* **2015**, *137*, 1400−1403.
(22) Yang, X.; Gitter, S. R.; Roessler, A. G.; Zimmerman, P. M.; Boydston, A. J. An Ion-Pairing Approach to Stereoselective Metal-Free Ring-Opening Metathesis Polymerization. *Angew. Chem., Int. Ed.* **2021**, *60*, 13952−13958.
(23) Lu, P.; Alrashdi, N. M.; Boydston, A. J. Bidirectional Metal-Free ROMP from Difunctional Organic Initiators. *J. Polym. Sci., Part A: Polym. Chem.* **2017**, *55*, 2977−2982.
(24) For a different mechanistic approach to metal-free ROMP, see: (a) Quach, P. K.; Hsu, J. H.; Keresztes, I.; Fors, B. P.; Lambert, T. H. Metal-Free Ring-Opening Metathesis Polymerization with Hydrazonium Initiators. *Angew. Chem., Int. Ed.* **2022**, *61*, No. e202203344. (b) Kellner-Rogers, J. S.; Hsu, J. H.; Keresztes, I.; Fors, B. P.; Lambert, T. H. Hydrazine-Catalysed Ring-Opening Metathesis Polymerization Of Cyclobutenes. *Angew. Chem., Int. Ed.* **2024**, *63*, No. e202413093.
(25) Kim, J.; Wu, C. J.; Kim, W.-J.; Kim, J.; Lee, H.; Kim, J.-D. Ring-Opening Metathesis Polymerization of Tetracyclododecene using Various Catalyst Systems. *J. Appl. Polym. Sci.* **2010**, *116*, 479−485.
(26) Lu, P.; Kensy, V. K.; Tritt, R. L.; Seidenkranz, D. T.; Boydston, A. J. Metal-Free Ring-Opening Metathesis Polymerization: From Concept to Creation. *Acc. Chem. Res.* **2020**, *53*, 2325−2335.
(27) Cater, H. L.; Balynska, I.; Allen, M. J.; Freeman, B. D.; Page, Z. A. User Guide to Ring-Opening Metathesis Polymerization of endo-Norbornene Monomers with Chelated Initiators. *Macromolecules* **2022**, *55* (15), 6671−6679.
(28) Jiang, L.; Nykypanchuk, D.; Ribbe, A. E.; Rzayev, J. One-Shot Synthesis and Melt Self-Assembly of Bottlebrush Copolymers with a Gradient Compositional Profile. *ACS Macro Lett.* **2018**, *7* (6), 619−623.
(29) Ogbonna, N. D.; Dearman, M.; Cho, C.; Bharti, B.; Peters, A. J.; Lawrence, J. Topologically Precise and Discrete Bottlebrush Polymers: Synthesis, Characterization, and Structure-Property Relationships. *JACS Au* **2022**, *2*, 898−905.
(30) Grigoriadis, C.; Nese, A.; Matyjaszewski, K.; Pakula, T.; Butt, T.; Floudas, G. Dynamic Homogeneity by Architectural Design − Bottlebrush Polymers. *Macromol. Chem. Phys.* **2012**, *213*, 1311−1320.
(31) Tsukahara, Y.; Namba, S. I.; Iwasa, J.; Nakano, Y.; Kaeriyama, K.; Takahashi, M. Bulk Properties of Poly(macromonomer)s of Increased Backbone and Branch Lengths. *Macromolecules* **2001**, *34*, 2624−2629.
(32) Khalyavina, A.; Häußler, L.; Lederer, A. Effect of the Degree of Branching on the Glass Transition Temperature of Polyesters. *Polymer* **2012**, *53*, 1049−1053.

https://doi.org/10.1021/acsmacrolett.5c00300
ACS Macro Lett. 2025, 14, 983−988